Taming Jets in magnetized fluids

Y. Kosuga[1] and N. H. Brummell[2]

[1)] *Center for Astrophysics and Space Sciences and Department of physics, University of California at San Diego, 9500 Gilman Drive, La Jolla, CA 92093*

[2)] *Department of Applied Mathematic and Statistics, University of California at Santa Cruz, 1156 High Street, Santa Cruz, CA 95064*

Effects of a uniform horizontal magnetic field on jets dynamics in 2D Boussinesq turbulence, i.e. Howard-Krishnamurti problem are studied with a numerical simulation. For a fixed fluid and magnetic diffusivity, it is shown that as the imposed field strength becomes larger jets start behaving in a more organized way, i.e. achieve stationary state and are finally quenched. The time evolution of total stress, Reynolds stress, Maxwell stress is examined and all the stresses are shown to vanish when jets are quenched. The quenching of jets is confirmed for different values of magnetic diffusivity, albeit the required field strength increases. It is also shown that the inclusion of overstable modes reinforces jets where Maxwell stress overcomes Reynolds stress. For a larger imposed field jets are shown to quench. A possible mechanism for the transition to the reinforcement of jets by Maxwell stress is discussed based on the transition in the most unstable mode in the underlying turbulence.

I. INTRODUCTION

Turbulence and subsequent turbulence driven large scale flows or Jets are ubiquitous phenomena in nature. In the convective region in the sun, turbulence is driven by the convective instability and the differential rotation result[1]. In planets, the Jupiter or the earth for example, geostrophic turbulence with Rossby waves is excited due to the energy input from the Sun, etc, and produces the famous zonal bands of Jets, i.e. zonal flows[2,3]. The combination of turbulence and large scale flows are observed in laboratory plasmas as well. In tokamaks, a device to confine plasmas magnetically, inhomogeneity in temperature or density excites drift wave turbulence and the drift wave turbulence in turn produces large scale flows called intrinsic rotation[4,5] and zonal flows[6,7], which are analogous to the differential rotation in the sun and zonal jets on planets, respectively. Understanding basic physics of these systems with turbulence and jets is an important issue, since of course these systems are physically interesting and challenging to model, but also are quite beneficial from a practical point of view: in fusion devices these large scale flows are believed to play an important role to achieve better confinement by reducing turbulent transport of heat and particle and improving stability of tokamak plasmas.

To be more specific, we focus on the issue of the generation and quenching of jets in 2D turbulence with magnetic field. A theory for beta plane MHD turbulence was formulated[8] and numerical work[9] was done to confirm the quenching of jets by the inclusion of magnetic field in beta plane turbulence; however, they used arbitrary forcing to excite turbulence. Here, instead, we consider a problem of jets dynamics in 2D *convective* turbulence, which is a natural forcing mechanism, with *horizontal* magnetic field, where horizontal here means the direction of jets which is normal to the direction with a temperature gradient. The problem with a vertical magnetic field, i.e. the problem of the magneto-convection was treated and understood fairly well[10–12]. The research of jets in 2D convective turbulence *without* magnetic field was pioneered by Krishnamurti et al[13] who observed the tilting of convective cell, formation of jets, chaotic motion which destroys well-defined structures of cells, by increasing the Rayleigh number for different values of the Prandtl number. Here the Rayleigh number measures the strength of temperature difference in a system and the Prandtl number is defined to be the ratio of a fluid viscosity and a thermal diffusivity. Howard et al[14] modeled the phenomena as a dynamical system with truncated Fourier components which

includes the famous Lorenz system for convection as a subsystem. The transition between different flow patterns was described as the transition between fixed points and especially the transition from steady convective cell to jets with tilted steady cells was understood as an instability of the fixed point which represents a steady convective solution. Numerical experiments also confirmed the similar behavior and further discovered different type of behavior such as a pulsating traveling wave[15]. The problem was extended to include a horizontal magnetic field and understand the transition of flow patterns discovered by the simulation for 2D convective turbulence with compressibility (anelastic approximation) and a horizontal magnetic field[16,17]. They observed the transition of flow patterns from a chaotic pattern to conductive state where the instability is switched off, by increasing the Chandrasekhar number[18] $Q \equiv v_A^2 d^2/(\nu\eta)$ at a *fixed* Rayleigh number. However, the result is somewhat trivial, since the increasing of the Chandrasekhar number or the increasing of the field strength for a fixed magnetic diffusivity, leads to the stabilization of the linear convective instability, the very source which drives rich behaviors in the system, i.e. the formation of jets, oscillation of jets and so on. And also the dynamics of jets, which is the main focus in this report, was not the focus of the work by Lantz et al.

In this report, we examine the effect of horizontal magnetic fields on the transition between flow patterns in 2D convective turbulence, i.e. Howard & Krishnamurti (HK) problem. We especially focus on the behavior of jets, i.e. whether horizontal magnetic fields weaken, quench, or possibly enhance jets. In doing so, we start from HK problem with a given parameter set, and change the values of the horizontal magnetic field imposed on a system and magnetic diffusivity, *with a fixed criticality*. First we focus on the cases without overstable modes, which exist only when $\eta > \kappa$, where η and κ is magnetic diffusivity and thermal conductivity respectively, and show that the jets are quenched by increasing the Chandrasekhar number. We calculate the balance between Reynolds stress and Maxwell stress for different values of Q and show that Reynolds stress always exceeds Maxwell stress. Hence the jets are quenched due to the cancellation of Reynolds stress by Maxwell stress. We also show the results with different magnetic diffusivities and show that qualitative picture of jets quenching agree with those obtained by Tobias et al[9]. We also calculate the case when overstable modes exist in a system and show that Maxwell stress can exceed Reynolds stress for high enough Q. We give an 'guesstimation' for the value of the transition between Reynolds stress driven regime and Maxwell stress regime.

The reminder of the report is organized as follows. In the section 2 we review the set of equations, conservation relations, and linear stability problems to identify important parameters in the system and different modes possible one could have. In the section 3, we show the simulation results on the dynamics of jets with the horizontal magnetic fields. The section 4 is conclusions and discussions.

II. FORMULATION

In this section we give the set of equations for 2D Boussinesq system with a horizontal magnetic field and review basic properties of them. Specifically we give a brief discussion on the conserved quantities in the system and linear stability problem. For the conservation relations, we discuss the conservation of energy, magnetic potential and cross helicity. Of these we pay a special attention to magnetic potential and cross helicity, which leads to Zeldvich theorem and a local conservation of momentum between waves and flows, respectively. For the stability problem, we derive dispersion relations for critical modes and show that there are two possibilities for the onset of the instability; one is a stationary cell which is analogous to the usual hydrodynamic convection and the other is an overstabile mode which is unique to the Rayleigh-Benard convection with magnetic fields. Some of the discussions given here are beyond the scope of the report, but I just do it any way since it would be helpful for me to summarize them!

A. 2D Boussinesq system with a uniform horizontal magnetic field

We consider a simple 2D Boussinesq system with a uniform horizontal magnetic field. As a coordinate system, we take x being the horizontal direction, y being the neglected direction, z being the vertical direction with temperature difference. We consider a box with a height d in z, a length L in x. The set of equations are momentum, temperature and induction equations:

$$\partial_t \mathbf{v} + \mathbf{v}\cdot\nabla\mathbf{v} = -\frac{1}{\rho}\nabla p_{tot} - \left(1+\frac{\delta\rho}{\rho}\right) g\hat{z} + \frac{1}{4\pi\rho}\mathbf{B}\cdot\nabla\mathbf{B} + \nu\nabla^2\mathbf{v} \tag{1}$$

$$\partial_t T + \mathbf{v}\cdot\nabla T = \kappa\nabla^2 T \tag{2}$$

$$\partial_t \mathbf{B} = \nabla\times(\mathbf{v}\times\mathbf{B}) + \eta\nabla^2\mathbf{B} \tag{3}$$

where $\delta\rho/\rho = -\alpha(T - T_0)$ denotes the effect of density variation due to the thermal expansion, which leads to the buoyant force. Introducing the stream function and magnetic potential to write $\mathbf{v} = \hat{y} \times \nabla\psi$, $\mathbf{B} = \hat{y} \times \nabla A$ (since $\nabla \cdot \mathbf{v} = \nabla \cdot \mathbf{B} = 0$), taking curl of the equation of motion and integrating induction equation we can rewrite the equations as

$$\partial_t \nabla^2 \psi + J(\psi, \nabla^2 \psi) = g\alpha \partial_x T + \frac{1}{4\pi\rho} \mathbf{B} \cdot \nabla \nabla^2 A + \nu \nabla^2 \nabla^2 \psi \tag{4}$$

$$\partial_t T + J(\psi, \theta) = \kappa \nabla^2 T \tag{5}$$

$$\partial_t A + J(\psi, A) = \eta \nabla^2 A \tag{6}$$

where $J(A, B) \equiv \partial_x A \partial_z B - \partial_z A \partial_x B$. Setting $T = T(z) + \theta'$ and $A = -B_0 z + A'$, where the prime denotes a fluctuation part of physical quantities, we get

$$\partial_t \nabla^2 \psi' + J(\psi', \nabla^2 \psi') = \sigma R \partial_x \theta' + \sigma\zeta Q \partial_x \nabla^2 A' + \sigma\zeta Q J(A', \nabla^2 A') + \sigma \nabla^4 \psi' \tag{7}$$

$$\partial_t \theta' + J(\psi', \theta') = \partial_x \psi' + \nabla^2 \theta' \tag{8}$$

$$\partial_t A' + J(\psi', A') = \partial_x \psi' + \zeta \nabla^2 A' \tag{9}$$

Here the physical quantities are normalized as $t \to t/(\kappa^{-1} d^2)$, $l \to l/d$, $\theta \to \theta/\Delta T$ ($\Delta T \equiv d|\partial_z T(z)|$), $A' \to A'/dB_0$ and the dimensionless numbers are the Prandtl number $\sigma \equiv \nu/\kappa$, the Rayleigh number $R \equiv g\alpha \Delta T d^3/(\nu\kappa)$, the magnetic Prandtl number $\zeta \equiv \eta/\kappa$ and the Chandrasekhar number $Q \equiv B_0^2 d^2/(\nu\eta 4\pi\rho)$.

We take periodic boundary condition in the horizontal direction. In the vertical direction, we consider stress free, i.e. $\psi = \partial_z^2 \psi = 0$ at $z = 0, 1$ and perfect conductor both in thermal and electric, i.e. $\theta' = B_z' = \partial_x A' = 0$ at $z = 0, 1$.

The set of equations conserves energy $\int d^2x \{(\nabla\psi)^2 + \sigma\zeta Q (\nabla A)^2\}$, magnetic potential squared $\int d^2x A^2$ and cross helicity $\int d^2x \mathbf{v} \cdot \mathbf{B}$. The energy conservation can be derived by multiplying ψ to the vorticity equation and $\nabla^2 A$ to the equation for the magnetic potential, which yields

$$\begin{aligned} &\partial_t \int d^2x \left\{ \frac{(\nabla\psi')^2}{2} + \sigma\zeta Q \frac{(\nabla A')^2}{2} \right\} \\ =&\sigma R \int d^2x w'\theta' - \sigma \int d^2x (\nabla^2 \psi')^2 - \sigma\zeta^2 Q \int d^2x (\nabla^2 A')^2 \end{aligned} \tag{10}$$

Note the boundary terms vanish by the boundary conditions. The first term in the right hand side is the turbulent heat flux, the second and the third terms in the right hand side

are the dissipation in ψ and A, respectively. Note that the turbulent flux is positive definite as can be shown from the temperature equation:

$$\partial_t \int d^2x \frac{\theta'^2}{2} = \int d^2x w'\theta' - \int d^2x (\nabla\theta')^2 \tag{11}$$

For a stationary state, one has

$$\int d^2x w'\theta' = \int d^2x (\nabla\theta')^2 > 0 \tag{12}$$

This is physically plausible since the temperature difference is such that the bottom is hot and the top is cold, which would yield the heat flux from the bottom to the top, i.e. the positive heat flux. Given the positivity of the heat flux, a stationary state is possible by balancing the right hand side of the energy equation as

$$\sigma R \int d^2x w'\theta' = \sigma \int d^2x (\nabla^2\psi')^2 + \sigma\zeta^2 Q \int d^2x (\nabla^2 A')^2 \tag{13}$$

which states that the turbulent flux resulting from temperature relaxation must be balanced with the dissipation in the kinetic and magnetic energy.

The conservation of the magnetic potential squared also has a non-trivial consequence. The conservation reads

$$\partial_t \int d^2x \frac{A'^2}{2} = \int d^2x w' A' - \zeta \int d^2x (\nabla A')^2 \tag{14}$$

which for a stationary state yields

$$\int d^2x w' A' = \zeta \int d^2x (\nabla A')^2 \tag{15}$$

In a dimensional form, we have

$$\int d^2x w' A' = \frac{\eta_{col}}{B_0} \int d^2x (\nabla A')^2 \tag{16}$$

Note that the left hand side is the turbulent flux of magnetic potential which can be written $-\eta_{turb}\partial_z\langle A\rangle = \eta_{turb} B_0$ where η_{turb} is the turbulent resistivity. From this, one can derive the Zeldovich theorem

$$\frac{\eta_{turb}}{\eta_{col}} = \frac{\int d^2x B'^2}{\int d^2x B_0^2} \tag{17}$$

which states that a large root mean square of magnetic fluctuations results when a turbulent transport dominates collisional, i.e. $\eta_{turb} \gg \eta_{col}$. We will use the theorem later.

The conservation of the cross helicity is related to momentum conservation. Using the Elsasser variable $\mathbf{z}_\pm \equiv \mathbf{v} \pm \mathbf{B}/4\pi\rho$, which describes the population of Alfven waves propagating in opposite directions along a large scale magnetic field, one can write

$$4\mathbf{v}\cdot\mathbf{B} = \mathbf{z}_+^2 - \mathbf{z}_-^2 \tag{18}$$

So the cross helicity is tied to the imbalance between the population density propagating in opposite directions, which suggests the role of the cross helicity as the momentum of waves, since if more waves propagate in one direction then waves would have a finite value of the momentum in the direction. To explicitly see the momentum balance, we derive a *local* conservation theorem, i.e. we integrate only over the horizontal direction x. A global conservation would be a trivial one due to the fact that $\int dz U(z) = 0$ where $U(z)$ is a mean flow in the horizontal direction. Multiplying A to the vorticity equation and $\nabla^2\psi$ to the magnetic potential equation, integrating only over x and dropping the third order terms in fluctuations, one has

$$\begin{aligned}\partial_t\langle A'\nabla^2\psi'\rangle =& -\sigma R\langle B_z'\theta'\rangle + \sigma\langle A'\nabla^4\psi'\rangle + \zeta\langle\nabla^2 A'\nabla^2\psi'\rangle \\ &+ \langle\partial_x\psi'\nabla^2\psi'\rangle - \sigma\zeta Q\langle\partial_x A'\nabla^2 A'\rangle\end{aligned} \tag{19}$$

Here $\langle ...\rangle \equiv L^{-1}\int dx$ is an ensemble average over a statistical distribution of fluctuating quantities. The ensemble average and the spatial integration in the horizontal direction is equivalent by assuming the ergodicity. Note the Taylor identity[19] relates the last two terms to the Reynolds and Maxwell stress, since

$$\begin{aligned}\langle\partial_x\psi'\nabla^2\psi'\rangle =& \left\langle \partial_x\frac{(\partial_x\psi')^2}{2} + \partial_z(\partial_x\psi'\partial_z\psi') - \partial_x\frac{(\partial_z\psi')^2}{2}\right\rangle \\ =& -\partial_z\langle w'u'\rangle\end{aligned} \tag{20}$$

Similarly $\langle\partial_x A'\nabla^2 A'\rangle = -\partial_z\langle B_z'B_x'\rangle$. Substituting these relations we have

$$\begin{aligned}\partial_t\langle A'\nabla^2\psi'\rangle =& -\sigma R\langle B_z'\theta'\rangle + \sigma\langle A'\nabla^4\psi'\rangle + \zeta\langle\nabla^2 A'\nabla^2\psi'\rangle \\ &- \partial_z\langle w'u' - \sigma\zeta Q B_z'B_x'\rangle\end{aligned} \tag{21}$$

The mean flow evolution is given by

$$\partial_t\langle U(z)\rangle + \partial_z\langle w'u' - \sigma\zeta Q B_z'B_x'\rangle = \sigma\partial_z^2\langle U(z)\rangle \tag{22}$$

Combining the two equations, we have the local balance of the cross helicity, or the momentum balance, as

$$\partial_t(\langle U\rangle - \langle A'\nabla^2\psi'\rangle) = \sigma R\langle B_z'\theta'\rangle - \sigma\langle A'\nabla^4\psi'\rangle - \zeta\langle\nabla^2 A'\nabla^2\psi'\rangle + \sigma\partial_z^2\langle U\rangle \tag{23}$$

So flow and waves or turbulence can exchange momentum with each other. Here, more precisely, the momentum is conserved between a flow and *a gas of Alfven waves* which is described by Elsasser variables. The momentum theorem has the structural similarity as the non-acceleration theorem first derived for the momentum balance between a large scale flow and gravity waves[20]; in the absence of the forcing (here $\langle B_z'\theta'\rangle$) and the dissipation in turbulence, one cannot accelerate flow with a stationary turbulence. The theorem also predicts a stationary profile of the flow:

$$\begin{aligned}\langle U(z)\rangle =& \langle U(0)\rangle \\ &- \int_0^z dz' \int_0^{z'} dz'' \left(R\langle B_z'\theta'\rangle - \langle A'\nabla^4\psi'\rangle - \frac{\zeta}{\sigma}\langle\nabla^2 A'\nabla^2\psi'\rangle \right)\end{aligned} \tag{24}$$

The flow profile is determined by the forcing and dissipation profile. Note that the *global* conservation of the cross helicity follows by integrating over the vertical direction z, i.e.

$$\partial_t \int d^2x \nabla\psi'\cdot\nabla A' = \sigma R\int d^2x B_z'\theta' - (\sigma+\zeta)\int d^2x\nabla^2\psi'\nabla^2 A' \tag{25}$$

The mean flow contribution drops due to the boundary condition.

B. Linear stability

Before going into the detail on the transition of flow patterns and jets dynamics, it would be useful to review the role of magnetic fields in the linear instability problem. The boundary conditions allow one to write solutions in the form

$$\psi = \mathrm{Re}\sum_k \hat{\psi}_k e^{-i\omega t + ik_x x}\sin k_z z \tag{26}$$

θ' and A' are also in the same form. Substituting the expression into the set of equations, linearizing them and requiring the marginality ($\mathrm{Im}(\omega) = 0$), we get two solutions.

The one of the solutions is the steady cell solution given by

$$\omega = 0 \tag{27}$$

$$R = \frac{k^6}{k_x^2} + Qk^2 \tag{28}$$

where $k^2 \equiv k_x^2 + k_z^2$. This solution corresponds to the famous Rayleigh-Benard convection[18] if $Q = 0$. Note that the critical Rayleigh number for the instability increases as Q increases, i.e. the mode is stabilized. Q increases when i) the strength of the imposed field B_0 increases or ii) the magnetic diffusivity η decreases. The case i) makes the bending of field lines more difficult: as field strength increases the 'rigidity' or 'elasticity' of field lines increase, which leads to the stabilizing effect. The case ii) can be understood in terms of freezing-in law of field lines: as magnetic diffusivity decreases the freezing-in law becomes more effective, which makes fluids more susceptive to field lines.

The second solution is an overstable mode, which is given by

$$\omega^2 = \frac{1-\zeta}{1+\sigma}\sigma\zeta Q k_x^2 - \zeta^2 k^4 \tag{29}$$

$$R = \frac{(\sigma+\zeta)(\zeta+1)}{\sigma}\left(\frac{k^6}{k_x^2} + \frac{\zeta}{1+\zeta}\frac{\sigma}{1+\sigma}Qk^2\right) \tag{30}$$

Note that this solution exists only when $\zeta < 1$, i.e. when the magnetic field does not diffuse away while the temperature does. Note also that this mode reduces to the Alfven waves for a inviscid case: $\omega^2 \to v_A^2 k_x^2$ where $v_A^2 \equiv B_0^2/(4\pi\rho)$. Hence this mode is unique to magnetized systems and we will pay a special attention later.

The two different modes, i.e. stationary cells and overstable modes, have different critical Rayleigh number, which indicate the dominant mode changes dependent on the value of Q. For example, when $Q = 0$, the critical Rayleigh number becomes $R = k^6/k_x^2$ and $R = (1+\zeta/\sigma)(1+\zeta)k^6/k_x^2$. Hence the stationary cell is more unstable for a small value of Q. On the other hand, since $\zeta(\sigma+\zeta)/(\sigma+1) < 1$ for $\zeta < 1$, the critical Rayleigh number for the overstable mode increases less rapidly compared to the stationary cell as Q increases. Hence when the Chandrasekhar number is large enough, or the imposed field strength is large enough for a fixed magnetic diffusivity, the overstable mode becomes more unstable. The crossover of the two different regime with two different dominant modes occurs at

$$Q_{cross} = \frac{1+\sigma}{\sigma}\frac{\zeta}{1-\zeta}\frac{k^4}{k_x^2} \tag{31}$$

The relation between R and Q is summarized in the figure 1.

III. JETS

In this section we discuss the dynamics of the jets with magnetic fields. First we focus only on the effect of the horizontal fields on jets dynamics. In doing so, we fix the Prandtl

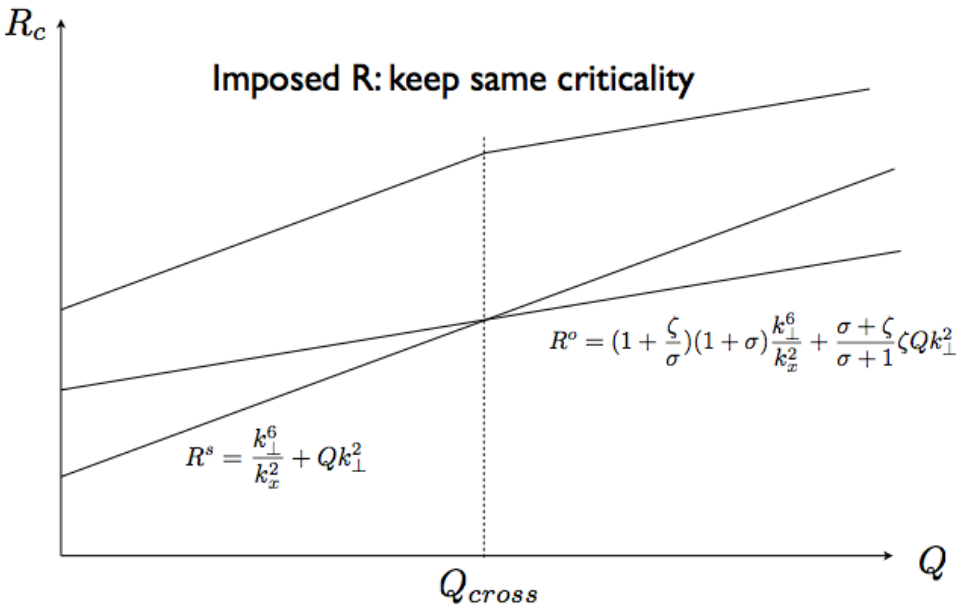

FIG. 1. the critical Rayleigh number as a function of Q. Stationary cell and overstable mode depend on Q differently. The stationary cell is dominant for small Q and the overstable modes are dominant for large Q. The crossover occurs at Q_{cross}. Even before the crossover value, the relative importance of the overstable modes increases.

number, the magnetic Prandtl number and the aspect ratio and vary the Chandrasekhar number and the Rayleigh number. The Rayleigh number is varied so that we keep the same criticality. Note that throughout the report the Prandtl number and the aspect ratio of the box is kept fixed to be $\sigma = 10$ and $\lambda \equiv L/d = 1/4$. The Prandtl number is chosen to be close to the experimental value[13]. The aspect ratio is chosen so that we can isolate $n_x = 1$ modes as an unstable modes from other n_x modes, where n_x is the mode number $k_x = 2\pi n_x/\lambda$. For example the critical Rayleigh number for hydrodynamic convection is $R = 417136$ for the $n_x = 1$ mode and $R = 6445817$ for the $n_x = 2$ mode and higher for the higher n_x. Given the parameters and starting from a fairly chaotic flow profile without a field, we show that jets start oscillating with an apparent periodicity in an organized manner, achieving stationary state and being quenched as magnetic field strength increases. After examining the jets dynamics with a varying field and fixed diffusivity, we examine the effect of different values of magnetic diffusivity. As the final topic, we include the overstable modes, i.e. we show the simulation results for a parameter range $\zeta < 1$ ($\zeta = 0.5$ here) and show that jets exhibit

interesting feature.

A. Taming jets with magnetic fields

Without magnetic field, jets exhibit complicated behavior[13–15]. Figure 2 is the simulation result for a unmagnetized case with $\sigma = 10$, $\zeta = 1$, $R = 660000$ and $Q = 0$. The critical value of the Rayleigh number for the onset of instability for this case is $R = 417136$. The aspect ratio of the box is fixed to be $\lambda \equiv L/d = 1/4$, which is a tall thin cell and isolates the $n_x = 1$ mode as the only linearly unstable mode. The simulation was over a few thermal diffusion time. In this case, the system shows fairly chaotic behavior. In the initial stage, the linear instability sets in and the total kinetic energy of the system increases. After the onset of the linear instability, the large scale flow starts growing slowly, as indicated by the growth of the kinetic energy in the mean flow. Although we can see the large scale flow is driven in this case, we immediately notice that the system never achieves stationarity. The direction of the flow is not fixed either, as indicated in the time evolution of the flow velocity at $z = 0.2$. For a certain duration of the time, the flow is in a positive direction at $z = 0.2$; however after a certain period of the time, flow flips its direction and the flow reversal occurs again later. The pattern of the cell is not well-defined as indicated in the contour plot.

When a magnetic field is imposed, the system start behaving 'well.' The figure 3 is the simulation result for $Q = 100.5$, $R = 7.23 \times 10^6$ and other parameters are fixed. Note the Rayleigh number was increased to keep the supercriticality constant. There exists a well-defined periodic oscillation. As in the unmagnetized case, the linear instability appears in the initial stage and subsequently the large scale flow gradually grows. Although the system behaves in a more organized way compared to the unmagnetized case, i.e. periodic oscillation as opposed to the chaotic behavior, the system does not achieve stationary state either. The flow still flips its direction, as indicated in the time evolution of the flow velocity or the instantaneous pattern of the flow and the cell. The cell exhibits well-defined structure, while changing the direction of the tilting at different times. Note that the spike in the total kinetic energy: the time of the spike corresponds to the time when the reversal of the flow occurs. We speculate this might be related to an instability in the large scale flow, i.e. Kelvin-Helmholtz type instability; however a clarification is ongoing and we do not go in detail further here.

When the imposed magnetic field increases, the system changes its behavior drastically: the system reaches stationarity. The figure 4 is the simulation result for $Q = 150$, $R = 7.56 \times 10^6$ and other parameters are fixed. As in the other cases, the linear instability occurs in the initial stage and the large scale flow grows after the onset of linear instability. After the growth of the large scale flow, a stationary state is achieved. A flow and cell pattern at a given time in the stationary state is shown in the figure 4. At the stationary state the flow and cell patterns are fixed and they maintain their structure. The magnetic field can organize the system, or make the jets behave well.

When the imposed magnetic field further increases, the jets are quenched, as indicated in the figure 5. The parameters used for the simulation were $Q = 200$, $R = 7.56 \times 10^6$ with other parameters fixed. The linear instability grows in the initial stage; however, the subsequent growth of the large scale flow is quenched. Note the supercriticality is same in the other cases as can be seen in the level of the total kinetic energy: Both $Q = 150$ and $Q = 200$ cases have the same turbulence level or the total kinetic energy $\sim 10^4$. Hence the jets are quenched while the linear instability is not. The pattern of the cell and flow is plotted in the figure 5 as well, which shows the well-defined structures of the convective cells. The magnetic field can quench the jets while the linear instability survives.

In summarizing, we considered the effect of the horizontal magnetic field to the formation of the jets in Howard-Krishnamurti problem, by varying Q and R while fixing other parameters including magnetic diffusivity. In the unmagnetized cases the large scale flow grows, while the system shows fairly complicated behavior. As the imposed magnetic field increases with a constant supercriticality, the jets i) start behaving in a more organized way, i.e. exhibit well-defined oscillation without achieving a stationary state, ii) achieve a stationary state with a stationary pattern in the cell and flow and iii) finally are quenched while the system is as unstable as other cases. This may be compared to the result obtained by Lantz[16] where they also observed the well-organized behavior of a system with an increasing magnetic field and quenching of the jets as well; however, they did not keep supercriticality fixed while Q was increased. Not surprisingly, then, the system starts behaving in a more organized way and jets are quenched since the system head toward *the linearly stable state*. Indeed in their numerical experiment the final state achieved as Q increased was the linearly stable state without the convection. Here, we kept the supercriticality constant, which indicates the quenching mechanism is different from the case by Lantz where the jets

are quenched partly because the linear instability is weakened. In the following, we try to identify the mechanism of the quenching of the jets.

So what is behind the view graphs? It is well known that the turbulent Reynolds stress can drive large scale flows. In magnetized fluids, in addition to the Reynolds stress, one has Maxwell stress which originates from the bending of the field lines. With these stresses the flow evolution is described as

$$\partial_t \langle U(z) \rangle + \partial_z \langle w'u' - \sigma\zeta Q B'_z B'_x \rangle = \sigma \partial_z^2 \langle U(z) \rangle \tag{32}$$

Here $\langle ... \rangle$ is defined in the same as before, i.e. $\langle ... \rangle = \int dx ...$ due ergodicity. Given the relation, it would be physically plausible to check the stress balance when the quenching occurs.

The figure 6 is the simulation results for different magnetic fields $Q = 130,\ 150,\ 170$ and shows the time evolution of Reynolds, Maxwell and total stresses at a given position ($z = 0.2$ here) with the corresponding cell patterns. Note all the cases are well-behaving system, i.e. the system which achieves stationarity. For $Q = 130$, Reynolds stress (red) exceeds Maxwell stress (green) and the total stress (blue) has the same sign as the Reynolds stress, which suggests the flow is Reynolds stress driven. The pattern of the cell is fixed and large scale flow profile is such that the flow is in left (negative x) at the top of the box and in right (positive x) at the bottom of the box. As the field strength increased to $Q = 150$, the system shows the similar behavior as in the case with $Q = 130$, while the tilting of the cell is weakened. The cancellation between Reynolds and Maxwell stresses becomes larger and the total driving becomes weaker. When the magnetic field strength is increased to $Q = 170$ the stresses cancel with each other and the neither of Reynolds or Maxwell stress has a finite value. Due to the cancellation of the stresses the large scale flows are quenched and the cell patterns are that of the convective cells without any flows. Note for a larger value of Q, say $Q = 500$, it was observed that the system behaves in the same way, i.e. the stresses cancel and both Reynolds and Maxwell stresses are suppressed for a stationary state with the standard convective cells.

Of course the relevant question to ask here is why the quenching occurs at the value of $Q = 170$. In order to estimate the value of Q for a quenching, we can do a 'back-of-an-envelope' type calculation, i.e. 'guesstimation' as follows. Since the quenching occurs, the

energy would be equipartitioned between kinetic and magnetic energy, as

$$|v'^2| \sim \sigma\zeta Q|B'^2| \tag{33}$$

The root mean squared of the magnetic field is related to the turbulent mixing of the magnetic potential via Zeldovich theorem as

$$\zeta \int d^2x|B'^2| = \int d^2x\partial_x\psi' A' \tag{34}$$

The magnetic potential would be mixed by the advection due to the convective cell, i.e.

$$A' \sim \tau_c\partial_x\psi' \sim (k_z|v'_z|_{rms})^{-1}\partial_x\psi' \tag{35}$$

where τ_c is a time scale that the turbulent velocity field advects magnetic potential, which can be estimated to be a turn over time here. Collecting the estimates, we have

$$Q \sim \frac{|v'^2|}{\sigma}\frac{k_z|v'_z|_{rms}}{|\partial_x\psi'|^2} \sim \frac{k^2}{k_x^2}k_z\frac{|v'_z|_{rms}}{\sigma} \tag{36}$$

For the parameters we used here, $\sigma = 10$, $k_z = \pi$, $k_x = 2\pi/\lambda = 8\pi$ and $|v'_z|_{rms}$ from the simulation results, we have

$$Q \sim 30 \tag{37}$$

which suggests we need a larger envelope, or another physics missing here. One possibility may be the quenching of the turbulent resistivity. When we treated the mixing of the magnetic potential we considered the kinematic problem, i.e. we treated the magnetic potential as a passive scalar. Since the magnetic potential affects the ambient turbulent velocity field via Lorentz force, the magnetic potential is an active scalar. When the effect of the magnetic potential as an active scalar is incorporated for the calculation of the turbulent resistivity, one could have a quenching factor[21] which could enhance the value of Q. Further investions are left as a future work.

B. Magnetic diffusivity

Up to this point, we examined the effect of the field strength on the dynamics of the jets, specifically, quenching of jets, with *a fixed magnetic diffusivity* or ζ; however, ζ could play an important role since the magnetic diffusivity control the 'degree' of freezing-in law.

Hence, in this subsection we discuss the effect of different values of magnetic diffusivity on the jets dynamics.

The figure 7 shows the relation between the strength of magnetic fields and the strength of the magnetic diffusivity. The line separates the region with and without jets, i.e. gives the strength of the field to quench the jets for a given value of a magnetic diffusivity. As magnetic diffusivity increases, the frozen-in law is broken and the flow and field are decoupled; hence it becomes harder to affect the jets with magnetic fields, which requires stronger field to suppress jets. The same tendency was obtained by Tobias et al[9], although they treated different systems, i.e. jets dynamics in beta plane MHD turbulence with an arbitrary forcing. Note that they confirmed the tendency over decades, while here we only confirmed from $\zeta = 1$ to $\zeta = 10$. Note also that we only considered the case for $\zeta \geq 1$ to exclude the overstable modes which are considered in the following.

C. Overstable mode

In this subsection, we show the simulation results with the overstable modes. We show the time evolution of Reynolds, Maxwell and total stresses and pattern of the cell for different values of Q and R, with $\sigma = 10$, $\zeta = 0.5$ and $\lambda = 1/4$ fixed. So here again we are interested in the change of the jets' behavior for different values of the imposed fields, with a special attention to the overstable modes in this subsection. It would be useful to recall that as Q increases the dominant unstable modes change from the stationary cell to the overstable modes. See the figure 1 for the details. The value of Q at the crossover is given by Eq.(31), whose value is $Q = 715.976$ for the parameters we chose.

The figure 8 is the results for $Q = 150,\ 200,\ 500$. Note that all the values are less than the crossover values; hence the dominant modes or most unstable modes are the stationary cells. In this case, the system shows the similar behavior as shown before, i.e. as the imposed field strength increases the jets start behaving well (although oscillates), achieves a stationary state and *try* to quench the jets, as seen in the time evolution in total stresses. The total stress, which is responsible for the driving of large scale flows, is determined by Reynolds stress, i.e. Reynolds stress is always larger than Maxwell stress. Maxwell stress tries to cancel Reynolds stress as the imposed field increases. The relation between Reynolds stress and total stress is apparent in the result for $Q = 150$. Although the stress or equivalently

the flow pattern shows the oscillation, the total stress (blue) always has the same sign as the Reynolds stress (red). Hence the flow is Reynolds stress driven.

Now what happens if the imposed field strength Q is around the crossover value? The figure 9 is the results for $Q = 600,\ 800,\ 1000$. Note that here we are around the cross over value where the most unstable mode changes from the stationary cell to the overstable mode. Plotted are the time evolution of Reynolds (red), Maxwell (green) and total (blue) stresses and the pattern of the cells. In these simulations, the system changes its behavior drastically, i.e. Maxwell stress overcomes Reynolds stress which was *not* observed in the other cases without overstable modes. As the imposed field strength increases the imbalance becomes more dominant. These are the large scale flows which are driven by *Maxwell* stresses.

Since the Maxwell stress dominates and the imbalance becomes more dominant as the imposed magnetic fields increases, one may ask what happens if we keep increasing the strength of the field. The figure 10 shows the results for $Q = 1100,\ 1300,\ 1500$. Plotted are the time evolution of stresses and the cell patterns. Note that in this regime the cell changes the direction of tilting as compared to the regime treated in the figure 9. Also stresses show different behavior from the last one. Although the total stress is still dominated by Maxwell stress, the imbalance becomes smaller as Q increases. And finally at the value of $Q = 1500$ jets are quenched, as seen in the straight cell pattern and the cancellation in the total stress.

Based on how large scale flows are driven or the behavior of the stresses, we can consider *three* distinct regimes. The first regime is Reynolds stress driven regime. This is the usual case, as observed in the other results in the former sections. In this regime Reynolds stress is always larger than Maxwell stress and Maxwell stress start canceling as the imposed field strength increases. Note that the magnetic field makes jets behaving in a more ordered way. The second regime is Maxwell stress driven regime, with the increasing unbalance in total stress as the imposed field strength increases. In this case Maxwell stress wins Reynolds stress and the flow is driven by Maxwell stress. The third regime is also Maxwell driven, while the total stress decreases as the imposed magnetic fields becomes larger. In this regime jets are finally quenched. The figure 11 shows the flow profile for the different regimes.

We speculate that the Maxwell stress driven regime is unique to the system with overstable modes, since this regime was only observed in the case $\zeta < 1$ where overstable modes exist. This is also physically plausible, since magnetic fields act as unstable restoring forces, which would possibly overcome Reynolds stresses. Given this assumption or speculation, we

can estimate the value of Q where the Maxwell stress wins Reynolds stress. Since overstale modes would be the cause of the Maxwell stress driven total stress, the transition occurs when the overstable modes become most dominant, i.e. when the overstable modes becomes more unstable than the stationary cell, which is around the crossover value of the $Q \sim 700$. The numerical result of the transition between Reynolds stress driven case and Maxwell stress driven case is between $Q \sim 500$ and $Q \sim 600$, which is comparable to the crossover value $Q \sim 700$. The possible explanation on the offset would be due to the fact that the overstable modes increases relative importance before the crossover value as shown in the figure 1. Hence the transition value of Q for the Maxwell stress driven regime would be shifted toward a smaller value of Q. An alternative explanation would be the onset of non-linear instability, where the finite amplitude fluctuation helps instability to set in, giving rise to the shift in the transition value.

There are the other two important Q values in the problem; one is for the transition between two different Maxwell stress driven regimes and the other is for the quenching of jets. The underlying physics to determine these Q values are currently under investigation.

IV. CONCLUSIONS AND DISCUSSIONS

In this report, we considered the dynamics of jets in 2D Boussinesq convective turbulence with a horizontal magnetic field. We discussed simple properties of 2D Boussinesq system with a uniform horizontal magnetic field and showed results from numerical experiments on transitions between flow patterns for different values of the Rayleigh number, the Chandrasekhar number and the magnetic Prandtl number. The Rayleigh number was changed to keep the criticality as constant. The rest of the parameters, the Prandtl number and the aspect ration of the box were kept constant throughout the numerical experiments. The principal results are:

1. Momentum theorem was derived between flows and waves as

$$\partial_t(\langle U\rangle - \langle A'\nabla^2\psi'\rangle) = \sigma R\langle B_z'\theta'\rangle - \sigma\langle A'\nabla^4\psi'\rangle - \zeta\langle\nabla^2 A'\nabla^2\psi'\rangle + \sigma\partial_z^2\langle U\rangle \qquad (38)$$

   in a small amplitude limit. To describe the momentum balance, the cross helicity is utilized. A physical interpretation of the cross helicity as wave momentum was

discussed. Using the momentum theorem, a stationary profile of the mean flow was predicted as

$$\langle U(z)\rangle = \langle U(0)\rangle - \int_0^z dz' \int_0^{z'} dz'' \left(R\langle B_z'\theta'\rangle - \langle A'\nabla^4\psi'\rangle - \frac{\zeta}{\sigma}\langle \nabla^2 A'\nabla^2\psi'\rangle \right) \tag{39}$$

2. By starting from a fairy complicated flow pattern in hydrodynamic case and increasing the Chandrasekhar number Q with the magnetic Prandtl number ζ fixed, we found that; a) for $100 \lesssim Q \lesssim 150$, flow pattern starts oscillating with a definite period. stationary state was not achieved. b) for $150 \lesssim Q \lesssim 200$ system achieves steady state with a tilted cell structure. c) for $150 \lesssim Q$ jets are quenched. We confirmed that the total stress, i.e. sum of Reynolds stress and Maxwell stress decreases as Q increases, and both Reynolds stress and Maxwell stress becomes zero when jets are quenched. A simple estimate for the Q value at the quenching gave $Q \sim 30$. Quenching of the turbulent resistivity was proposed as the explanation for the offset.

3. We repeated the above experiment for different values of the magnetic Prandtl number ζ. It was shown that a larger ζ requires a larger Q to quench jets, which shows a similar qualitative behavior to the jets in forced beta plane MHD turbulence[9]. The result was interpreted based on the idea of the freezing-in law for MHD systems.

4. Including overstable modes, it was shown that Maxwell stress can exceed Reynolds stress. A transition from Reynolds stress driven jets to Maxwell stress driven jets was argued based on a crossover of most unstable modes. A numerical value of Q at the crossover was calculated to be $Q \sim 700$ for the parameters we chose and shown to be close to the numerical value of $Q \lesssim 600$ at the transition between Reynolds stress dominated jets and Maxwell stress dominated jets. It was argued that the shift in the transition value would be due to the increasing relative importance of the overstable modes before the actual crossover.

Following is a few remarks on a caveat.

1. The Reynolds number in the simulation, which can be calculated a-posteriori, is $Re \sim 10$ in the simulations presented here. Further study with higher Reynolds number is desirable, to see the dynamics of jets in a strongly turbulent regime.

2. We only focused on the dynamics of jets. Obviously, the dynamics of the fields would be interesting to check. Preliminary results show that the field lines are expelled in the Maxwell stress driven regime and not expelled in the Reynolds stress driven regime. This raises the question on the underlying physics of the transition Maxwell stress driven jets to Reynolds stress driven jets, since both flux expulsion and overstable modes can result when $\zeta < 1$.

ACKNOWLEDGMENTS

We thank P.H. Diamond, M.R.E. Proctor, D.W. Hughes and J. Mak for stimulating discussions on the related and unrelated problems. One of the authors (Y.K.) also thank P. Garaud, E. Rosenblum, T. Wood, R. Stancliffe, J. McCaslin, A. Traxler and all other ISIMA participants for providing a great time during the summer school.

REFERENCES

[1]G. Rüdiger, *Differential rotation and stellar convection* (Gordon and Breach Science Publishers, 1989).

[2]P. B. Rhines, Chaos, **2**, 313 (1994).

[3]G. K. Vallis, *Atmospheric and Oceanic Fluid Dynamics* (Cambridge University Press, 2006).

[4]J. E. Rice, W. D. Lee, E. S. Marmar, P. T. Bonoli, R. S. Granetz, M. J. Greenwald, A. E. Hubbard, I. H. Hutchinson, J. H. Irby, Y. Lin, D. Mossessian, J. A. Snipes, S. M. Wolfe, and S. J. Wukitch, Nucl. Fusion, **44**, 379 (2004).

[5]P. H. Diamond, C. J. McDevitt, Ö. D. Gürcan, T. S. Hahm, and V. Naulin, Phys. Plasmas, **15**, 012303 (2008).

[6]A. Fujisawa, K. Itoh, H. Iguchi, K. Matsuoka, S. Okamura, A. Shimizu, T. Minami, Y. Yoshimura, K. Nagaoka, C. Takahasi, M. Kojima, H. Nakano, S. Oshima, S. Nishimura, M. Isobe, C. Suzuki, T. Akiyama, K. Ida, K. Toi, S. I. Itoh, and P. H. Diamond, Phys. Rev. Lett., **93**, 165002 (2004).

[7]P. H. Diamond, S. I. Itoh, K. Itoh, and T. S. Hahm, Nucl. Fusion, **47**, R35 (2005).

[8]D. W. Hughes, R. Rosner, and N. O. Weiss, *The Solar Tachocline* (Cambridge University Press, 2007).

[9]S. M. Tobias, P. H. Diamond, and D. W. Hughes, ApJ, **667**, L113 (2007).

[10]M. Proctor, (2003), duraham Review Volume, Chapter 11: Magnetoconvection.

[11]A. M. Rucklidge and P. C. Matthhews, Nonlinearity, **9**, 311 (1996).

[12]A. M. Rucklidge, M. Proctor, and J. Prat, Geophys. Astrophys. Fluid Dynamics, **100**, 121 (2006).

[13]R. Krishnamurti and L. N. Howard, Proc. Natl. Acad. Sci. USA, **78**, 1981 (1981).

[14]L. N. Howard and R. Krishnamurti, J. Fluid Mech., **170**, 385 (1986).

[15]N. H. Brummell and K. A. Julien, (1993?), unpublished.

[16]S. R. Lantz and R. N. Sudan, ApJ, **441**, 903 (1995).

[17]S. R. Lantz, ApJ, **441**, 925 (1995).

[18]S. Chandrasekhar, *Hydrodynamic and Hydromagnetic stability* (Dover, 1961).

[19]G. I. Taylor, Phils. Trans., **215**, 1 (1915).

[20]J. G. Charney and P. G. Drazin, J. Geophys. Research, **66**, 83 (1961).

[21]A. V. Gruzinov and P. H. Diamond, Phys. Plasmas, **2**, 6 (1995).

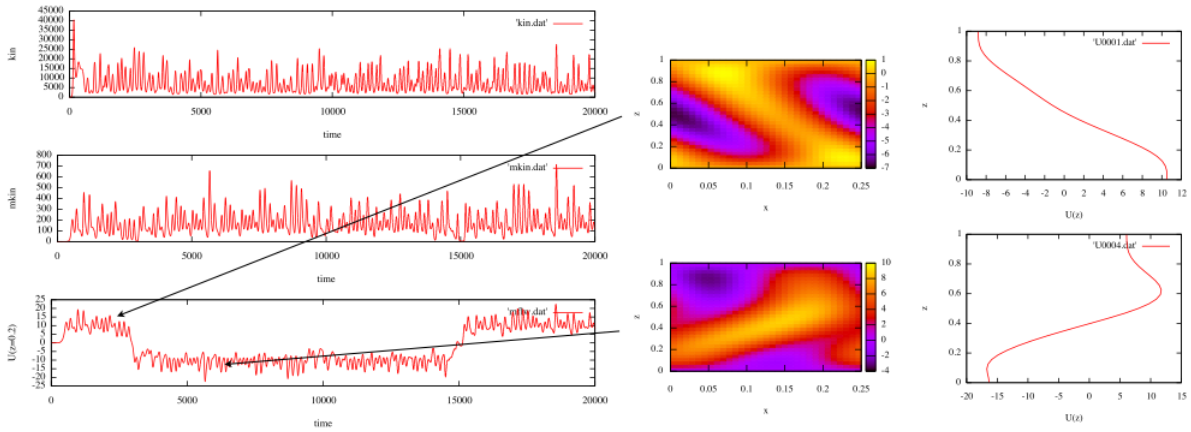

FIG. 2. Unmagnetized case. From upper left: time evolution of total kinetic energy. Middle left: time evolution of the kinetic energy in mean flow. Down left: time evolution of velocity at the position $z = 0.2$. Color: contour plot of stream function. Right: Flow profile corresponding to the contour plots

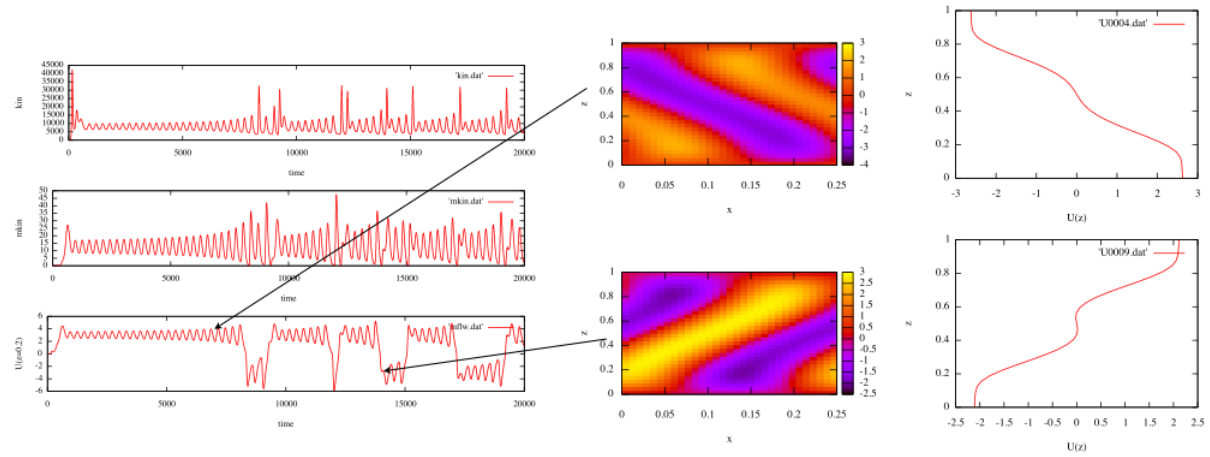

FIG. 3. With magnetic field $Q = 100.5$. From upper left: time evolution of total kinetic energy. Middle left: time evolution of the kinetic energy in mean flow. Down left: time evolution of velocity at the position $z = 0.2$. Color: contour plot of stream function. Right: Flow profile corresponding to the contour plots

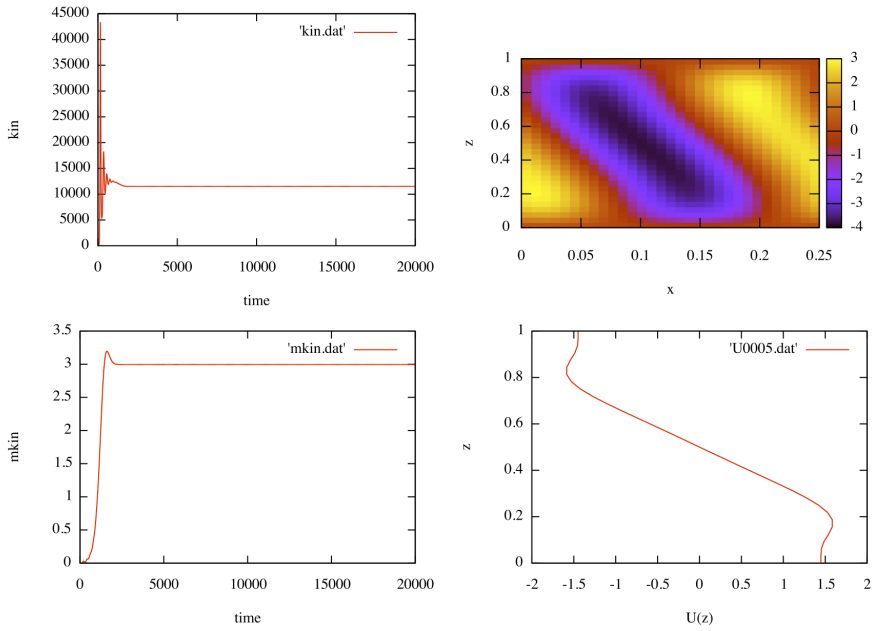

FIG. 4. With magnetic field $Q = 150$. From upper left: time evolution of total kinetic energy. Down left: time evolution of the kinetic energy in mean flow. Upper right: ontour plot of a stream function. Down right:Flow profile corresponding to the contour plot

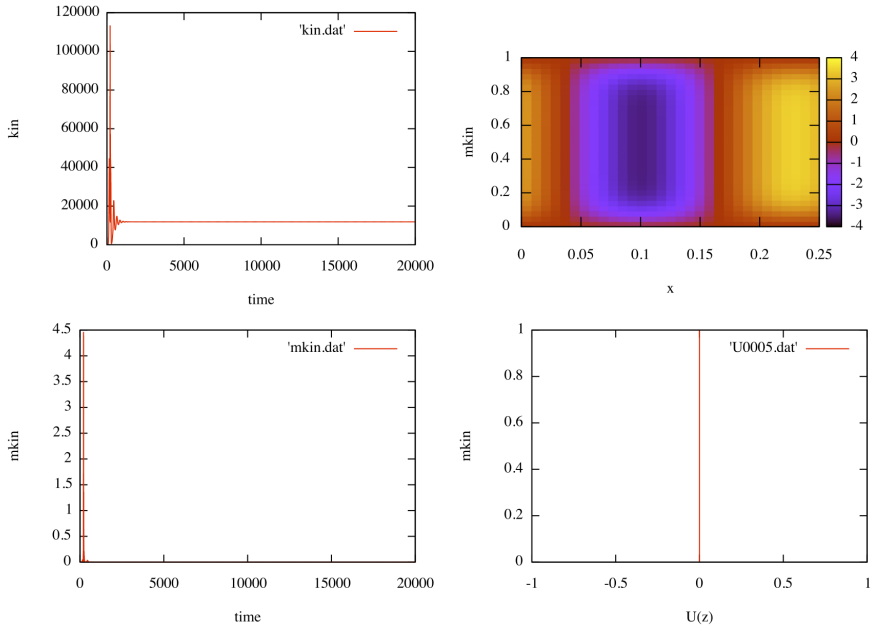

FIG. 5. With magnetic field $Q = 200$. From upper left: time evolution of total kinetic energy. Down left: time evolution of the kinetic energy in mean flow. Upper right: ontour plot of a stream function. Down right:Flow profile corresponding to the contour plot

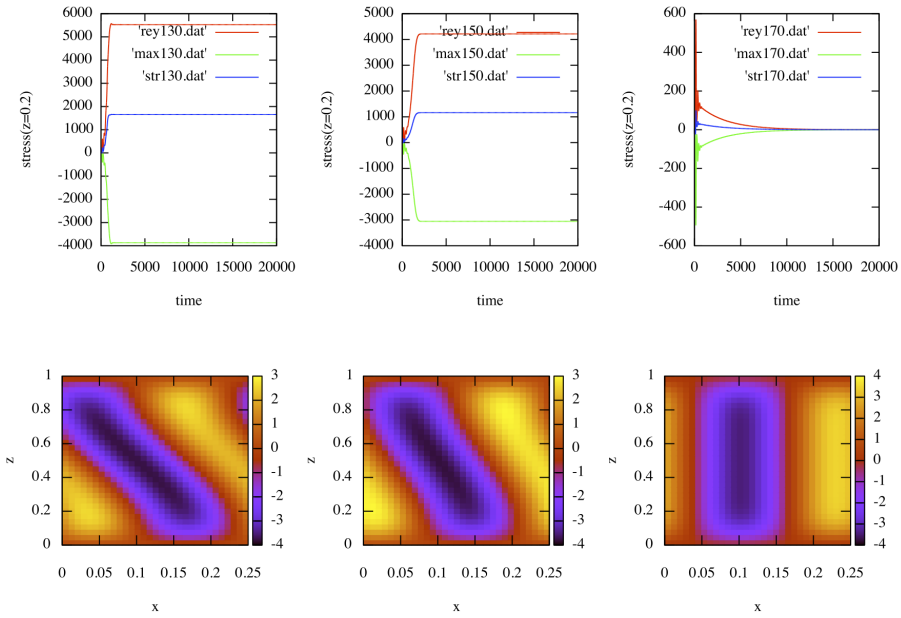

FIG. 6. From left to right, $Q = 130,\ 150,\ 170$ respectively. Up:Reynolds(red), Maxwell(green) and total(blue) stresses. Down: Contour plot of a stream function.

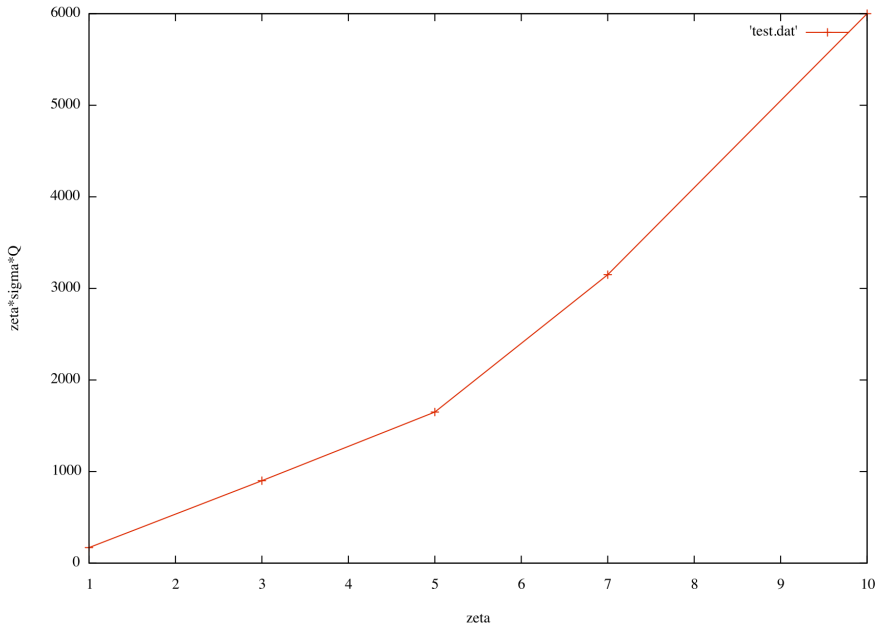

FIG. 7. The value of Q for quenching v.s. ζ. Above the line flows are quenched.

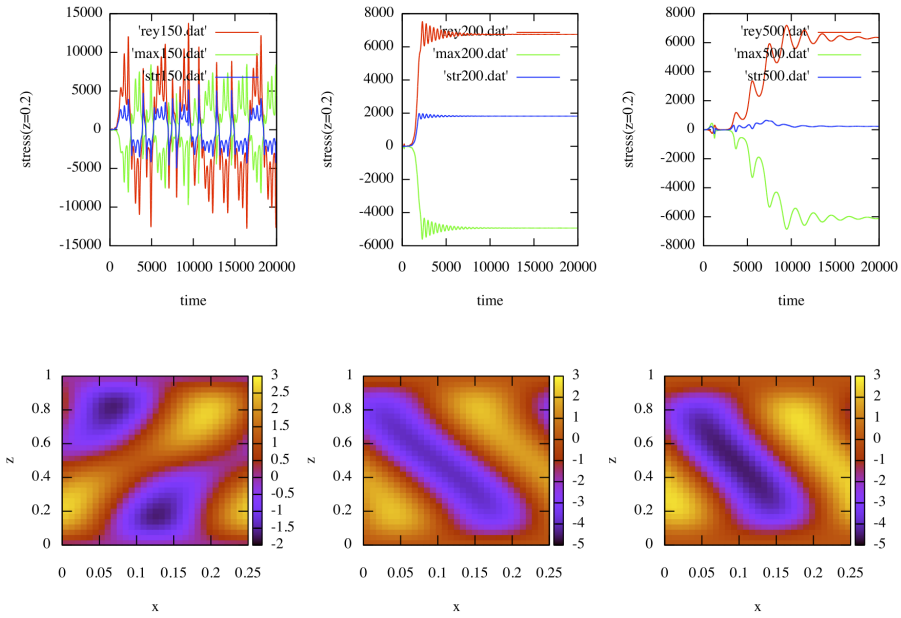

FIG. 8. From left to right, $Q = 150,\ 200,\ 500$ respectively. Up:Reynolds(red), Maxwell(green) and total(blue) stresses. Down: Contour plot of a stream function.

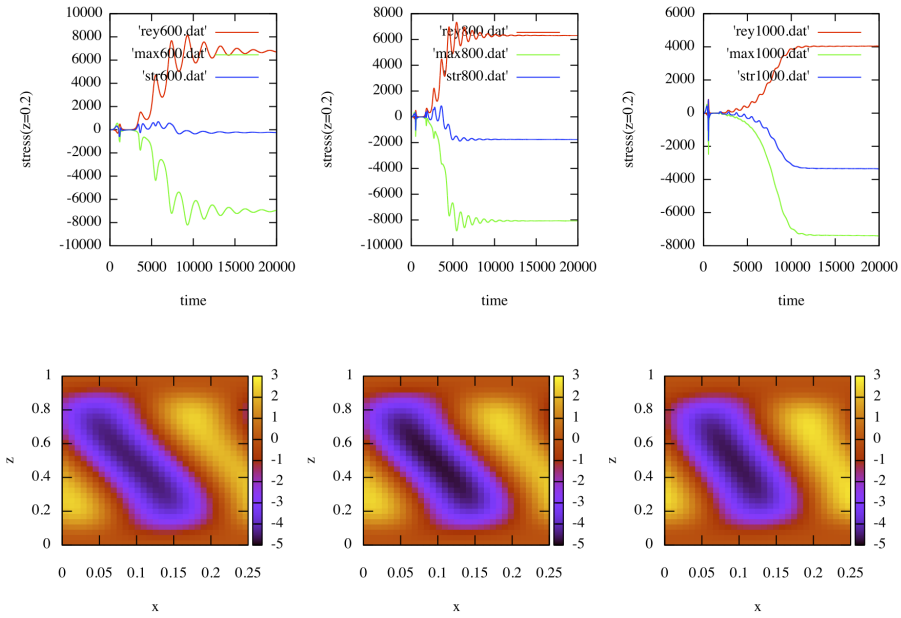

FIG. 9. From left to right, $Q = 600,\ 800,\ 1000$ respectively. Up:Reynolds(red), Maxwell(green) and total(blue) stresses. Down: Contour plot of a stream function.

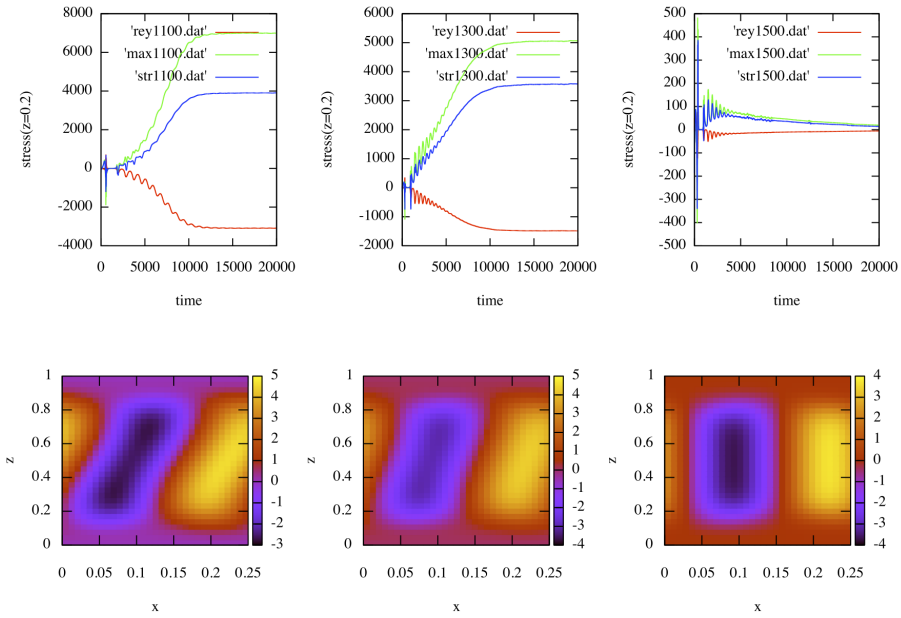

FIG. 10. From left to right, $Q = 1100,\ 1300,\ 1500$ respectively. Up:Reynolds(red), Maxwell(green) and total(blue) stresses. Down: Contour plot of a stream function.

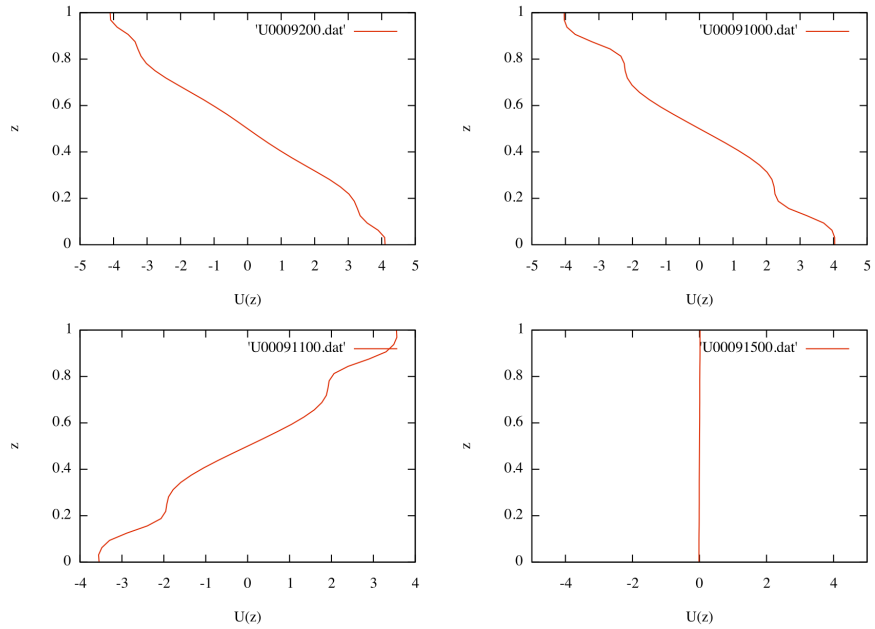

FIG. 11. Flow profile at different regimes. Upper left: Reynolds stress driven. Upper right: Maxwell stress driven. Down left: Maxwell stress driven. Down right: Cancellation of stresses and quenching of Jets.